# Supporting Information

## Honek et al. 10.1073/pnas.1415825111

### SI Materials and Methods

**Animals and Tissue Samples.** Animals were fasted for 4 h followed by euthanizing with a lethal dose of $CO_2$ and cervical dislocation. Blood samples were collected by intracardiac puncture after mice were killed. After euthanizing, s.c. white adipose tissue (scWAT) from the inguinal location, epididymal WAT (epiWAT), and interscapular brown adipose tissue (intBAT) were immediately dissected. For RNA isolation and protein extraction, adipose tissues were stored in liquid nitrogen and were subsequently transferred to −80 °C until further use as previously described (1, 2). Fresh tissues were fixed with 4% (wt/vol) paraformaldehyde overnight, washed with PBS, and either paraffin-embedded or proceeded for whole-mount immunohistochemical analysis.

**Treatments with Anti-VEGF and Anti-VEGF Receptor 2 Antibodies.** Mice at different ages were randomly divided into groups (about five animals per group). A rabbit anti-human and mouse VEGF neutralizing monoclonal antibody (Simcere Pharmaceuticals) (3, 4) and a rat anti-mouse VEGF receptor 2 (VEGFR2) neutralizing monoclonal antibody (ImClone Systems, Inc.) (4) were administered twice per week via i.p. injection for 4 wk at effective doses of 5 mg/kg and 200 μg/mouse, respectively. Vehicle-treated mice were used as controls.

**Antibodies.** Antibodies used in our study included a rat anti-mouse CD206 monoclonal antibody (Biolegend); a rat anti-mouse Endomucin monoclonal antibody (eBioscience); a rabbit anti-Iba1 polyclonal antibody (Wako Pure Chemicals Ltd.); a rat anti-mouse PECAM-1 (CD31) monoclonal antibody (BD Pharmingen); a guinea pig anti-Perilipin polyclonal antibody (Fitzgerald Industries International Inc.); a rabbit anti-mouse UCP1 antibody (Abcam); an anti-Prohibitin antibody (Abcam); a rat anti-mouse VEGF receptor 1 (VEGFR1) (MF1) antibody (ImClone Systems, Inc.); a rabbit anti-VEGFR-2 (T014) polyclonal antibody, kindly provided by Rolf A. Brekken, University of Texas Southwestern Medical Center, Dallas, TX; an Alexa-555 labeled goat anti-rat IgG (Molecular Probes); an Alexa-647–labeled goat anti-guinea pig IgG (Molecular Probes); an Alexa-555–labeled donkey anti-rabbit IgG (Molecular Probes), a Cy3-labeled Streptavidin (Jackson ImmunoResearch Laboratories, Inc.); a rabbit anti-VEGF monoclonal antibody (Simcere Pharmaceuticals); and a rat anti-mouse VEGFR2 (DC101) antibody (ImClone Systems, Inc.).

**H&E Staining.** Some tissue samples were stained with H&E using a standard protocol.

**Immunohistochemistry.** For whole-mount immunohistochemistry staining, small pieces of tissue samples (about 1 mm in thickness) were used as previously described (5, 6). Paraffin-embedded tissue as well as cryostat sections (5 μm thickness) were used for regular H&E and immunostaining.

Paraformaldehyde-fixed WAT and BAT samples were digested with 20 μg/mL proteinase K for 5 min, permeabilized with methanol, and stained at 4 °C overnight with a rat anti-mouse CD31 antibody (1:200). Subsequently, tissue samples were thoroughly washed and vascular endothelial cells were detected with an Alexa-555–labeled secondary antibody (1:200). After rigorous washing, samples were mounted in Vectashield mounting medium (Vector Laboratories, Inc.). Tissue samples were stored in the dark at −20 °C until examination using a confocal microscope (Zeiss confocal LSM510 microscope). Microimages of 6–10 randomized fields were collected from each tissue sample and analyzed using Adobe Photoshop CS5 software. Six images were used to compose the overlay with the separation of 5 μm between each layer.

Some adipose tissue samples were paraffin-embedded and sections were prepared in 5-μm thickness. Slides were stained with a guinea pig anti-perilipin antibody (1:400) and biotinylated isolectin-B4 (1:200) or a rabbit anti-mouse UCP1 (1:200). For isolectin-B4 staining, nonspecific binding sites were masked with an Avidin-Biotin-Blocking Kit (Vector Laboratories, Inc.). Positive signals were detected with a secondary goat anti-guinea pig Alexa-647–labeled antibody (1:400), a donkey anti-rabbit Cy3-labeled antibody (1:300), or with Cy3-labeled Streptavidin (1:300). Slides were mounted with Vectashield medium containing DAPI for nuclear staining (Vector Laboratories, Inc.) and stored at −20 °C until further examination. Microscopic images of 10–12 randomized fields were collected from each tissue sample and images were analyzed using Adobe Photoshop CS5 software.

For preparation of cryostat sections (5-μm thickness), some adipose tissue samples were embedded in the optimum cutting temperature compound Tissue-Tek (Sakura Finetek) and frozen on dry ice. Primary antibodies were incubated at 4 °C overnight, followed by detection with corresponding fluorescence-labeled secondary antibodies. Positive signals were detected using a confocal microscope.

**RNA Extraction and Quantitative Real-Time PCR.** WAT and BAT was homogenized using a VDI 12 Homogenizer (VWR International) and total RNA was isolated with a GeneJet RNA isolation kit (Thermo Fisher Scientific Inc.) according to the manufacturer's instructions. Briefly, 1.5 μg total RNA was reversely transcribed using a RevertAid H minus First Strand cDNA Synthesis Kit (Thermo Fisher Scientific Inc.) according to the manufacturer's protocol. For first-strand cDNA synthesis, a mixture of random hexamer nucleotides was used. Reverse transcription was performed at 42 °C for 60 min, followed by enzyme inactivation at 70 °C for 5 min. Samples were directly subjected to quantitative (q) RT-PCR using a StepOne Plus Real Time PCR system (Applied Biosystems) or stored at −20 °C until further use. A 20-μL reaction contained 10 μL SYBR Green reagent (Applied Biosystems), 150-nm forward and reverse primers, and 1 μL cDNA template. qRT-PCR was performed in duplicate and the protocol was executed for 40 cycles. Each cycle contained denaturation at 95 °C for 15 s, annealing at 60 °C for 1 min, and extension at 72 °C for 1 min. The primer pairs specific for different genes include the following: *mIl6* Sense: 5′-ATGGATGCTACCAAACTGGAT-3′, Anti-Sense: 3′-TGAAGGACTCTGGCTTTG TCT-5′; *mTnfa* Sense: 5′-ATGAGCACAGAAAGCATGATC-3′, Anti-Sense: 3′-TACAGGCTTGTCACTCGAATT-5′; *mVegfa* Sense: 5′-ATGAACTTTCTGCTCTCTT GGGT-3′, Anti-Sense: 3′-ACACAGGACGGCTTGAAGATGTA-5′; *mVegfr1* Sense: 5′-AGCCCACCTCTCTATCCGCTGG-3′, Antisense: 3′-GGCGCTTCCGAATCTCTAACG-5′; *mVegfr2* Sense: 5′-CTCTGTGGGTTTGCCTGGCGATTTTCT-3′, Antisense: 3′-GGGGATCACCACAGTTTTGTTCTTGTT-5′; *mUcp1* Sense: 5′-AA ACAGAAGGATTGCCGAAA-3′, Anti-Sense: 3′-TGCATTCTGACCTTCACGAC-5′; *mActin* Sense: 5′-AGGCCCAGAGCAAGAGAGG-3′, Anti-Sense: 3′-TACATGGCTGGGGTGTTGAA-5. Threshold cycle (Ct) values were obtained for all cDNA samples. As an internal control, the housekeeping gene actin was used. All calculated Ct values for the gene of interest were normalized to the Ct value of actin. The relative prevalence of transcripts was calculated using the 2-ΔΔCt method. The levels of

mRNA expression of genes were normalized to their respective control groups.

**ELISA.** Total protein fractions extracted from scWAT and epiWAT were used for immunodetection and mouse VEGF in adipose tissue lysates was quantified using a sensitive ELISA kit according to the manufacturer's instructions (R&D Systems).

**Intraperitoneal Insulin Tolerance Test.** For assessment of insulin sensitivity, female mice at the age of 1, 7, or 15 mo were fasted for 5 h with free access to drinking water. At the end of the fasting period, the baseline blood glucose levels (t = 0) were assessed with a glucometer (Accu-Chek Aviva; Roche Diagnostics). The tail vein of each mouse was punctured with a sterile needle and a drop of blood was applied to a glucose test strip.

For measuring i.p. insulin tolerance, 0.5 units of insulin were intraperitoneally injected into each mouse. A drop of blood was collected at 15, 30, 60, and 120 min after insulin injection and basal blood glucose levels were determined using a glucometer. For data analysis, the values were normalized based on the basal glucose level at t = 0. Changes in blood glucose are expressed as percentages relative to basal blood glucose.

**Blood Lipid, Glucose, and Insulin Measurements.** Serum samples from drug-treated and nontreated animals were prepared from blood collected from animals fasted for 5 h. Serum levels of cholesterol, glucose, glycerol, and triglycerides were determined using colorimetric assays (Abcam). Serum insulin levels were measured and quantified using a Mouse Insulin ELISA kit (Mercodia) and nonesterified free fatty acids were measured using a colorimetric assay (Wako Chemicals).

**Statistical Analysis.** Data of qPCR and blood lipids were presented as mean determinants (± SEM). The rest of data were shown as mean determinants (± SD). Statistical analysis was performed by the unpaired two-tailed Student *t* test using Microsoft Excel 2010.


1. Lim S, et al. (2012) Cold-induced activation of brown adipose tissue and adipose angiogenesis in mice. *Nat Protoc* 7(3):606–615.
2. Xue Y, Lim S, Bråkenhielm E, Cao Y (2010) Adipose angiogenesis: Quantitative methods to study microvessel growth, regression and remodeling in vivo. *Nat Protoc* 5(5):912–920.
3. Yang X, et al. (2013) Vascular endothelial growth factor-dependent spatiotemporal dual roles of placental growth factor in modulation of angiogenesis and tumor growth. *Proc Natl Acad Sci USA* 110(34):13932–13937.
4. Yang Y, et al. (2013) Anti-VEGF- and anti-VEGF receptor-induced vascular alteration in mouse healthy tissues. *Proc Natl Acad Sci USA* 110(29):12018–12023.
5. Hosaka K, et al. (2013) Tumour PDGF-BB expression levels determine dual effects of anti-PDGF drugs on vascular remodelling and metastasis. *Nat Commun* 4:2129.
6. Religa P, et al. (2013) VEGF significantly restores impaired memory behavior in Alzheimer's mice by improvement of vascular survival. *Sci Rep* 3:2053.

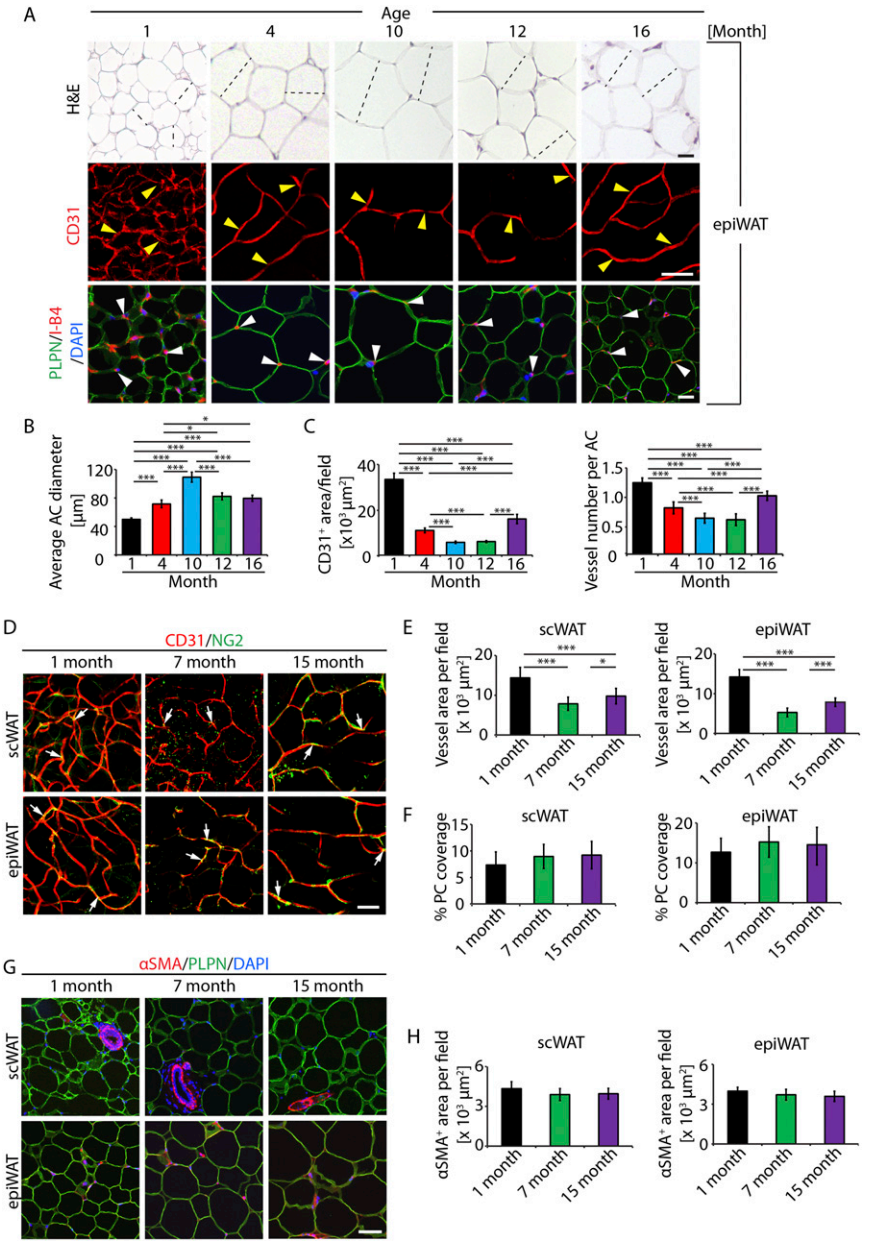


**Fig. S1.** Age-related changes of adipose vasculature and epiWAT adipocyte size and detection of NG2 and αSMA perivascular positive signals in scWAT and epiWAT. (*A*) Histology of adipocytes and vascular density of epiWAT. epiWATs were stained with H&E, CD31 (red), or perilipin (PLPN, green) plus isolectin B4 (I-B4, red) counterstained with DAPI (blue) nucleus staining. Arrowheads point to microvessels. Dashed lines show diameters of typical adipocytes. (Scale bars, 50 μm.) (*B*) Average diameters of adipocytes of epiWAT. Adipocyte sizes were quantified from 120 adipocytes from 12 fields. (*C*) Quantification of total microvessel density and numbers per adipocyte in epiWAT (12 fields per group). (*D*) CD31 and NG2 double immunostaining of scWAT and epiWAT of 1-, 7-, and 15-mo-old mice. Arrows indicate the adipose vasculature-associated $NG2^+$ pericytes. (Scale bar, 50 μm.) (*E*) Quantification of vessel density in scWAT and epiWAT of 1-, 7-, and 15-mo-old mice (12 fields per group). (*F*) Quantification of vascular coverage of $NG2^+$ pericytes (PC) in scWAT and epiWAT of 1-, 7-, and 15-mo-old mice (12 fields per group). (*G*) Triple immunostaining of scWAT and epiWAT of 1-, 7-, and 15-mo-old mice with αSMA (red), PLPN (green), and DAPI (blue). (*H*) Quantification of total $\alpha SMA^+$ signals in scWAT and epiWAT of 1-, 7-, and 15-mo-old mice (12 fields per group). $*P < 0.05$, $***P < 0.001$.

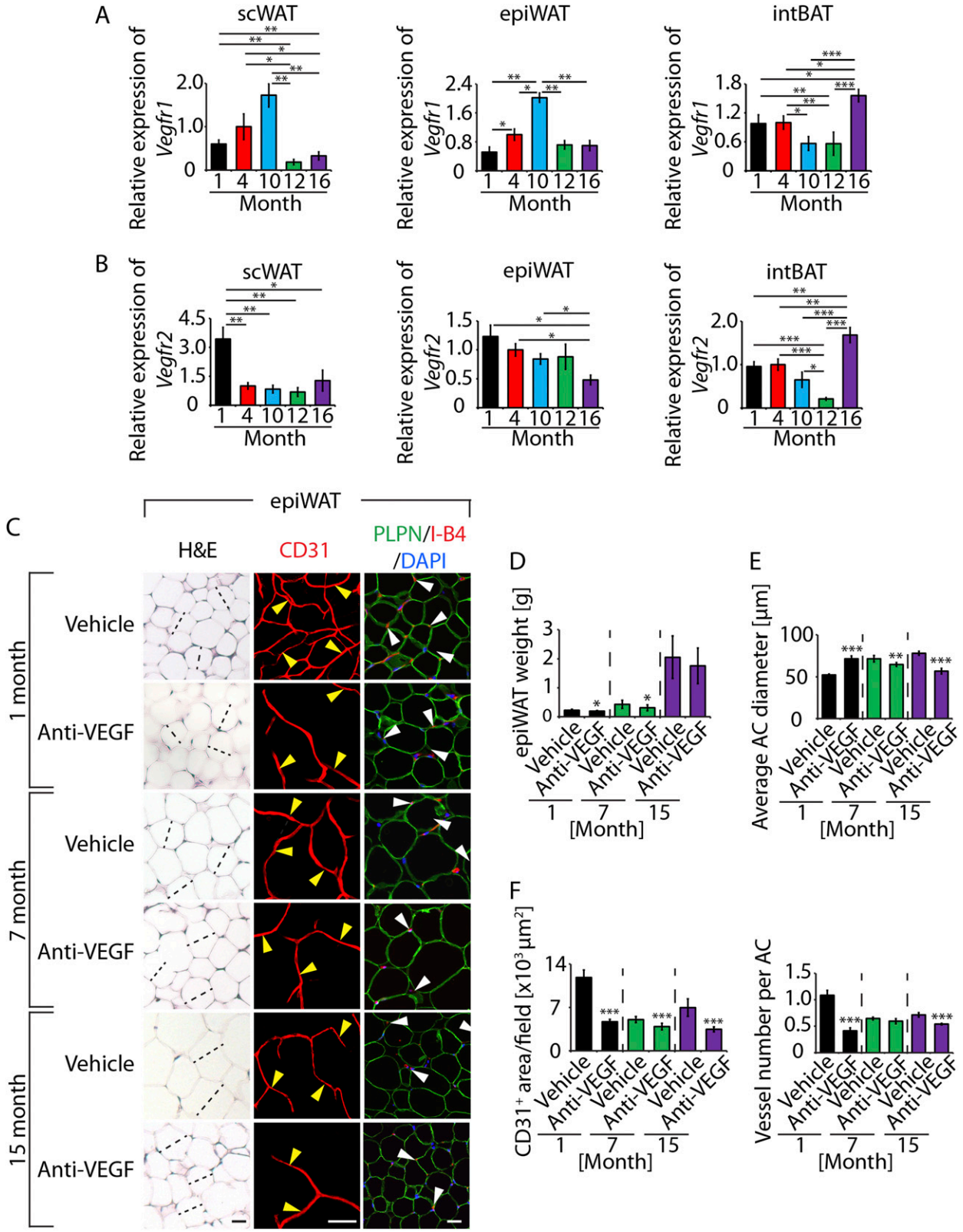


**Fig. S2.** Age-related changes in adipose vasculature and anti-VEGF therapy-induced vascular and adipocyte changes in epiWAT. (*A*) Quantification of *Vegfr1* mRNA expression by qPCR in scWAT, epiWAT and intBAT of various age groups (eight samples in duplicates per group). (*B*) Quantification of *Vegfr2* mRNA expression by qPCR in scWAT, epiWAT, and intBAT of various age groups (eight samples in duplicates per group). (*C*) Histology of adipocytes and vascular density of anti-VEGF– and vehicle-treated epiWAT. epiWATs were stained with H&E, CD31, or PLPN (blue) plus I-B4 (red) counterstained with DAPI (blue). Arrowheads point to microvessels. Dashed lines show diameters of typical apocytes. (Scale bars, 50 μm.) (*D*) Total weight of epiWAT of anti-VEGF– and vehicle-treated 1-, 7-, and 15-mo-old mice ($n$ = 10–18). (*E*) Average diameters of anti-VEGF– and vehicle-treated epiWAT adipocytes. Adipocyte sizes were quantified from 120 adipocytes from 12 fields. (*F*) Quantification of total microvessel density and numbers per adipocyte in anti-VEGF– and vehicle-treated epiWAT (12 fields per group). $^{*}P < 0.05$, $^{**}P < 0.01$, $^{***}P < 0.001$.

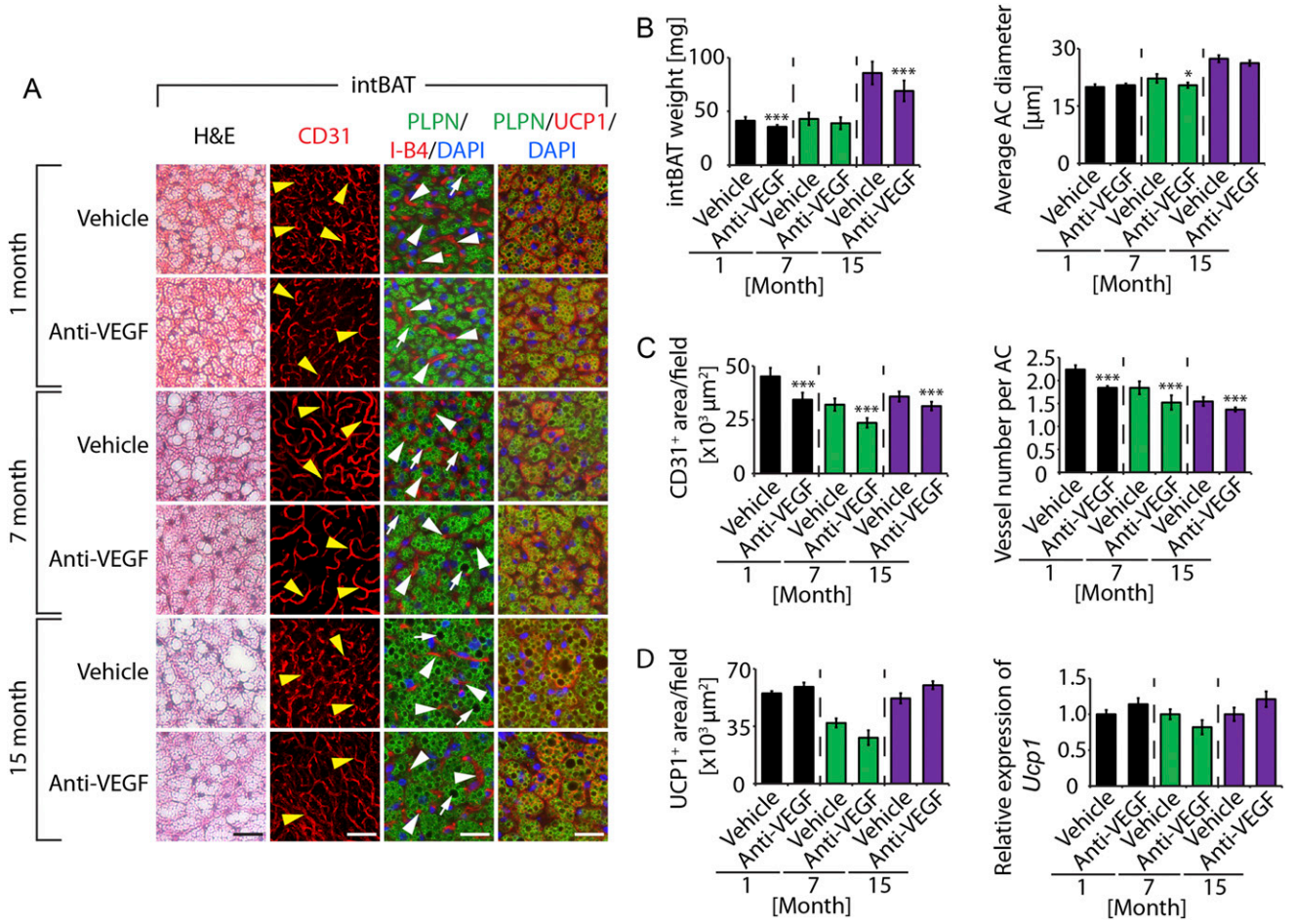


**Fig. S3.** Anti-VEGF therapy-induced vascular and adipocyte changes in intBAT. (*A*) Histology and immunohistochemistry of anti-VEGF– and vehicle-treated intBAT adipocyte sizes and vascular density in different age groups. Interscapular BAT was stained with H&E, CD31, or PLPN (blue) plus I-B4 (red) counter-stained with DAPI (blue) nucleus staining. UCP1 (red), PLPN (green), and DAPI triple staining is shown. Arrowheads point to microvessels and arrows point to lipid droplets. (Scale bars, 50 μm.) (*B*) Total weight of intBAT of anti-VEGF– or vehicle-treated 1-, 7-, and 15-mo-old C57BL/6 mice that were fed with normal chow ($n$ = 10–18). Average diameters of intBAT adipocytes and adipocyte sizes were quantified from 120 adipocytes from 12 fields of 10–18 animals. (*C*) Quantification of total vascular density and numbers per adipocyte in intBAT (12 fields per group). (*D*) Quantification of UCP1 protein-positive signals (12 samples per group). Quantification of *Ucp1* mRNA expression by qPCR (six to eight samples in duplicates per group). $*P < 0.05$, $**P < 0.01$, $***P < 0.001$.

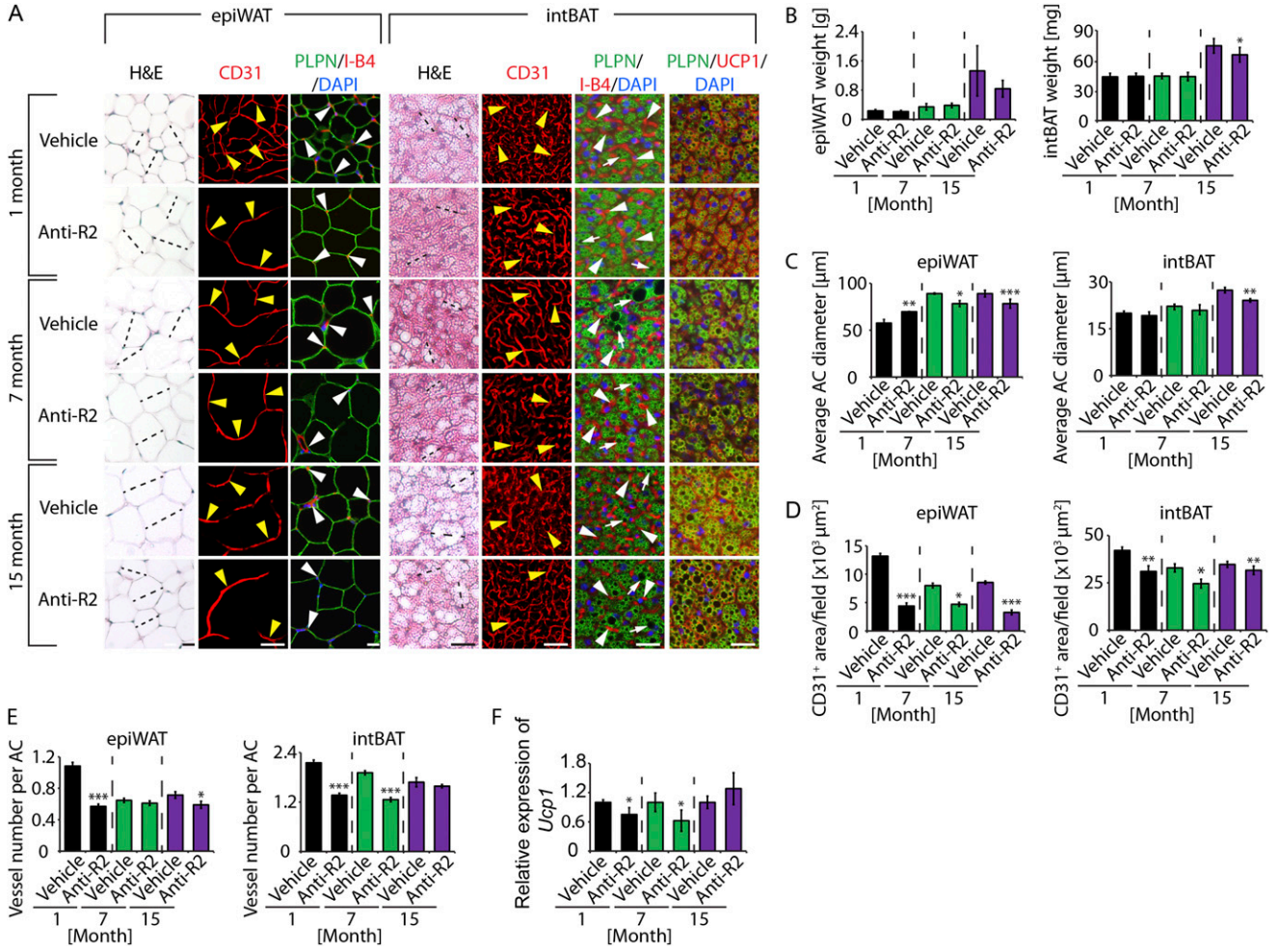


**Fig. S4.** Anti-VEGFR2 therapy-induced vascular and adipocyte changes in epiWAT and intBAT. (*A*) Histology and immunohistochemistry of anti-R2– and vehicle-treated epiWAT and intBAT adipocyte sizes and vascular density in different age groups. epiWAT and intBAT were stained with H&E, CD31, or PLPN (green) plus I-B4 (red) counterstained with DAPI (blue) nucleus staining. UCP1 (red), perilipin (green), and DAPI triple staining is shown. Dashed lines show diameter of typical adipocytes. Arrowheads point to microvessels and arrows point to lipid droplets. (Scale bars, 50 μm.) (*B*) Total weight of epiWAT and intBAT of anti-R2– or vehicle-treated 1-, 7-, and 15-mo-old C57BL/6 mice that were fed normal chow ($n = 10$). (*C*) Average diameters of epiWAT and intBAT adipocytes; adipocyte sizes were quantified from 120 adipocytes from 12 fields of 10 animals. (*D*) Quantification of total vascular density in epiWAT and intBAT (12 fields per group). (*E*) Quantification of microvessel numbers per adipocyte in epiWAT and intBAT (12 fields per group). (*F*) Quantification of *Ucp1* mRNA expression in intBAT by qPCR (six to eight samples in duplicates per group). $*P < 0.05$, $**P < 0.01$, $***P < 0.001$.

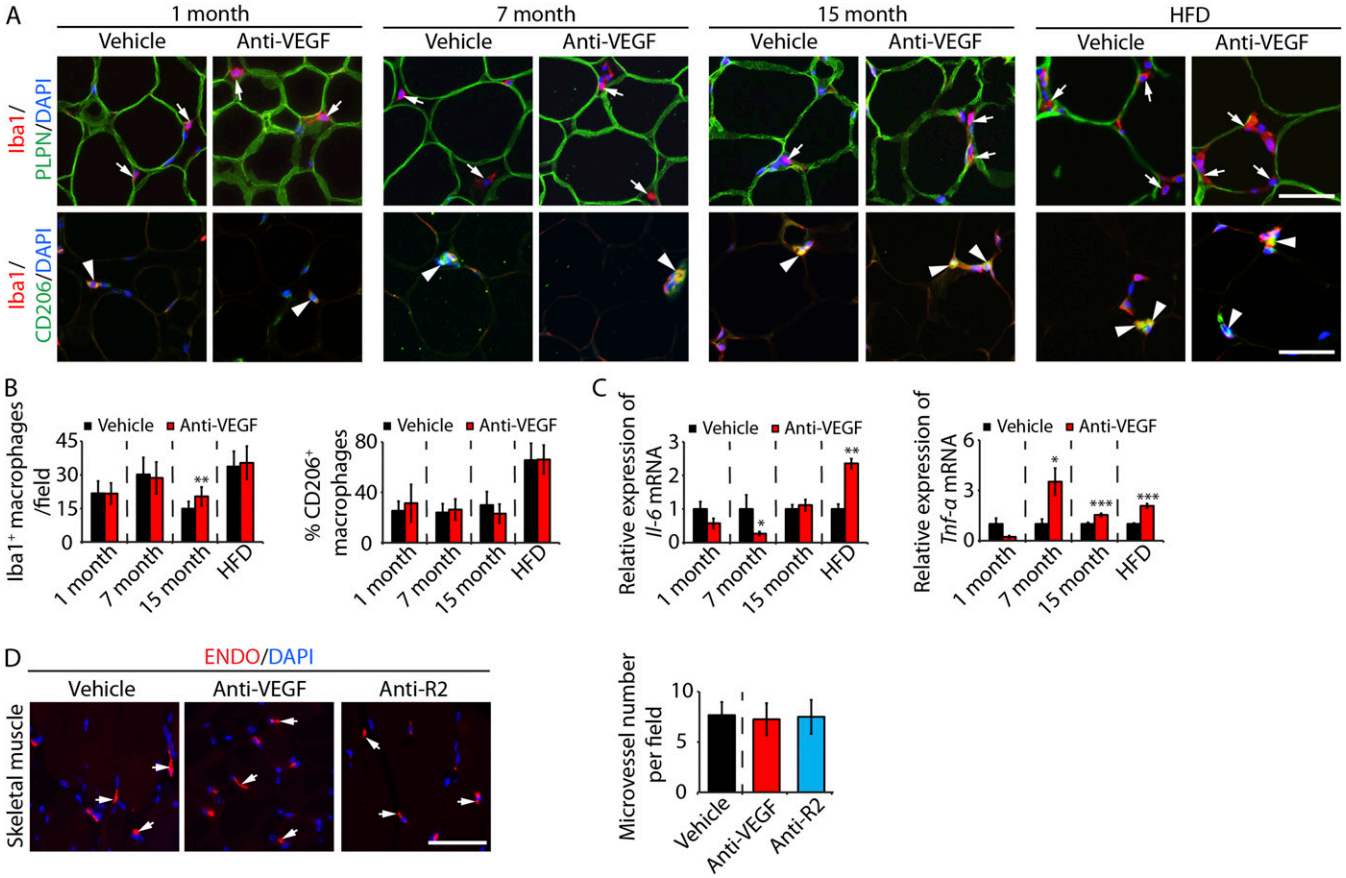


**Fig. S5.** Localization and quantification of macrophages in epiWAT and microvessels in skeletal muscle. (*A*) Immunohistochemical localization of Iba1$^+$ and CD206$^+$ macrophages in vehicle- and anti-VEGF–treated epiWAT of 1-, 7-, and 15-mo-old mice and 7-mo-old mice fed a high-fat diet (HFD). Arrows point to Iba1$^+$ macrophages; arrowheads indicate Iba1 and CD206 double-positive signals. PLPN staining marks adipocytes. (Scale bars, 50 μm.) (*B*) Quantification of Iba1$^+$ and CD206$^+$ macrophages in vehicle- and anti-VEGF–treated epiWAT of 1-, 7-, and 15-mo-old mice and 7-mo-old HFD-fed mice (12 fields per group). (*C*) qPCR quantification of *Il-6* and *Tnf-α* mRNA expression levels of vehicle- and anti-VEGF–treated epiWAT of 1-, 7-, and 15-mo-old mice and 7-mo-old HFD-fed mice (eight samples per group). (*D*) Immunohistochemical staining of vehicle-, anti-VEGF–, or anti-R2–treated quadriceps skeletal muscle tissue with ENDO (red). Arrows indicate ENDO$^+$ signals. The number of microvessels was counted from 12 fields per group. (Scale bars, 50 μm.) $^*P < 0.05$, $^{**}P < 0.01$, $^{***}P < 0.001$.

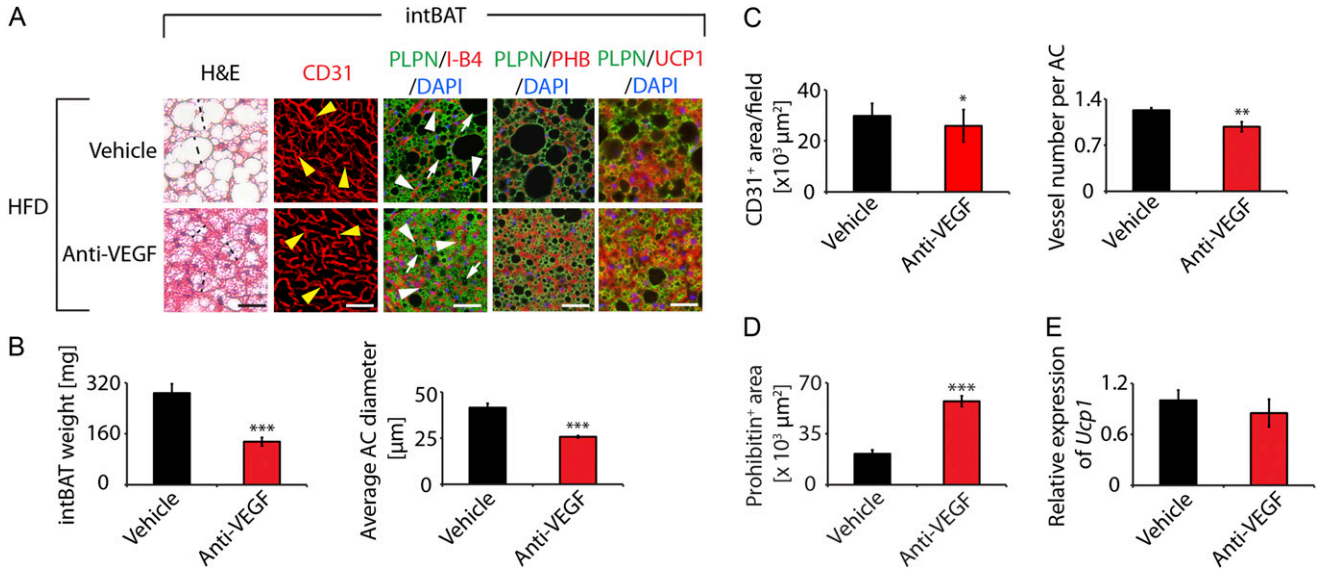


**Fig. S6.** Anti-VEGF treatment-induced vascular and adipocyte changes in intBAT of lean and obese mice. (*A*) Histology and immunohistochemistry of anti-VEGF and vehicle-treated intBAT adipocyte sizes and vascular density in lean and obese mice. Interscapular BAT was stained with H&E, CD31, or PLPN (green) plus I-B4 (red) counterstained with DAPI (blue) nucleus staining. UCP1 (red), PLPN (green) and DAPI triple staining is shown. Arrowheads point to microvessels and arrows point to lipid droplets. (Scale bars, 50 μm.) (*B*) Total weights of intBAT of anti-VEGF- and vehicle-treated HFD-fed 7-mo-old C57BL/6 mice ($n = 10$); $^{***}P < 0.001$. Average diameters of intBAT adipocytes and adipocyte sizes were quantified from 120 adipocytes from 12 fields of 10 animals; $^{***}P < 0.001$. (*C*) Quantification of total vascular density (*Left*) and numbers per adipocyte (*Right*) in intBAT (12 fields per group); $^{*}P < 0.05$, $^{**}P < 0.01$. (*D*) Immunohistochemical localization and quantification of prohibitin$^{+}$ mitochondria in vehicle- and anti-VEGF-treated intBAT of 7-mo-old HFD-fed obese mice. $^{***}P < 0.001$. (*E*) Quantification of *Ucp1* mRNA expression by qPCR (six samples in duplicates per group).